Dalton Transactions

Accepted Manuscript

ROYAL SOCIETY OF CHEMISTRY

www.rsc.org/dalton

Cite this: DOI: 10.1039/c0xx00000x

www.rsc.org/xxxxxx

ARTICLE TYPE

Anion complexation, transport and structural studies of a series of bis-methylurea compounds

Martina Olivari,[a] Riccardo Montis,[a] Louise E. Karagiannidis,[b] Peter N. Horton,[b] Lucy K. Mapp,[b] Simon J. Coles, [b] Mark E. Light,[b] Philip A. Gale,[b,*] and Claudia Caltagirone[a*]

Received (in XXX, XXX) Xth XXXXXXXXX 20XX, Accepted Xth XXXXXXXXX 20XX
DOI: 10.1039/b000000x

A new family of bis-methylureas (**L**[1]-**L**[6]) have been synthesised and their ability to bind anions both in solution and in the solid state and to transport them through lipid membrane have been studied. From the solid state studies it has emerged that various conformations can be adopted by the receptors allowing the isolation of complexes of different stoichiometry (from 1:1 to 1:3). The transport studies highlighted the possibility to use the bis-methylureas to mediate Cl^- transport across membranes.

1. Introduction

Bis-urea compounds have been used extensively for anion recognition. In 1995, Umezawa and co-workers[1] reported that bis-ureas and thioureas, obtained by the reaction of 1,3-bis(aminomethyl)benzene with butylisocyanate and butylisothiocyanate, showed some affinity for $H_2PO_4^-$ (K_a = 820 M^{-1} for the thiourea derivative) in DMSO-d_6. The same group also studied the application of phenyl-substituted ureas as an ionophore for the fabrication of anion selective electrodes with remarkable sulfate selectivity.[2] More recently Sellergren and co-workers studied the recognition of tyrosine phosphorylated peptides by the vinylphenyl urea derivative of 1,3-bis(aminomethyl)benzene.[3] Caltagirone and co-workers have recently reported the pyrophosphate optical sensing properties of 1,3-bis(aminomethyl)benzene and 2,6-bis(aminomethyl)pyridine derivatives bearing naphthalene and 2-nitrobenzene moieties.[4]

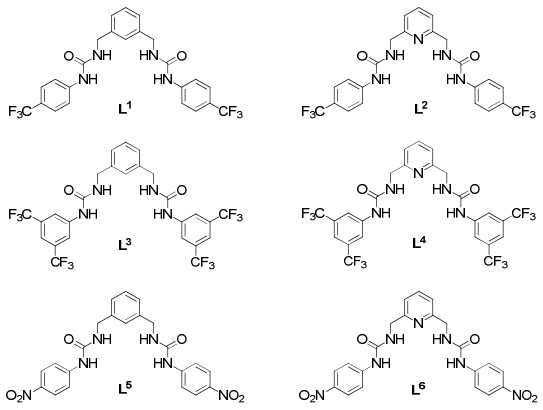

Scheme 1 Representation of receptors **L**[1]-**L**[6].

Gale and co-workers have previously shown that *ortho*-phenylenediamine-based bis-ureas are highly effective anion transport motifs with chloride transport activity observed at concentrations as low as 1:1000000 transporter to lipid molar ratio.[5] Gale has also shown that tripodal tren-based tris ureas and thioureas are capable of facilitating chloride/nitrate and chloride/bicarbonate antiport processes in POPC-based vesicles.[6] We, therefore, decided to study bis-ureas prepared from 1,3-bis(aminomethyl)benzene and 2,6-bis(aminomethyl)pyridine (see receptors **L**[1]-**L**[6] in scheme 1) as potential anion transporters due to their structural similarity to systems mentioned above. Therefore a series of 1,1'-(1,3-phenylenebis(methylene))bis(3-phenylureas) and 1,1'-(pyridine-2,6-diylbis(methylene))bis(3-phenylureas) were synthesized with electron withdrawing nitro and trifluoromethyl substituents which had previously been shown to enhance the transport properties of urea-based anion transporters.[5]

2. Results and Discussion

2.1. Synthesis and solid-state characterisation of receptors L[1]-L[6]

Compounds **L**[1], **L**[3], and **L**[5] were synthesised by the reaction of the commercially available 1,3-bis(aminomethyl)benzene reacted with the appropriate isocyanate (4-(trifluoromethyl)phenyl isocyanate, 3,5-bis(trifluoromethyl) phenyl isocyanate and 4-nitrophenyl isocyanate) in refluxing dichloromethane in the presence of triethylamine under nitrogen to give the three receptors in 70-97% yield. In the case of compounds **L**[2], **L**[4], and **L**[6] we first synthesised the 2,6-bis(amino-methyl)pyridine hydrochloride salt by a Delepine reaction of 2,6-bis-

Cite this: DOI: 10.1039/c0xx00000x

www.rsc.org/xxxxxx

ARTICLE TYPE

Table 1 Basic Crystallographic parameters

	CCDC	Crystal System (space group)	a (Å)	b (Å)	c (Å)	β (°)	V (Å^3)	Z
L^3-DMSO	1016980	*monoclinic (C2/c)*	26.454(2)	12.7445(9)	8.9389(5)	94.842(3)	3002.9(4)	4
L^4-MeOH	1016982	*monoclinic (C2/c)*	26.210(7)	12.739(3)	8.981(2)	96.618(5)	2978.7(13)	4
L^4-A	1016981	*monoclinic (P2/c)*	11.4364(9)	12.8183(10)	9.0313(7)	100.463(2)	1301.9(2)	2
L^1-AcO$^-$ (1:2)	1016983	*monoclinic (I2/a)*	34.550(2)	8.796(1)	43.222(3)	91.801(4)	13128.2(14)	8
L^3-AcO$^-$(1:2)	1016984	*monoclinic(I2/a)*	19.111(1)	8.420 (1)	42.107(3)	96.582(5)	6731.0(9)	4
L^3-CO$_3^{2-}$ (2:1)	1016985	*orthorhombic (Pbca)*	20.944(3)	24.898(3)	38.318(5)	90	19981(5)	8
L^4-HPO$_4^{2-}$(2:1)	1016986	*monoclinic (P2$_1$/n)*	12.536 (2)	32.550(4)	23.279(3)	97.732(2)	9413(2)	4
L^2-SO$_4^{2-}$ (3:1)	1016987	*monoclinic (P2$_1$/c)*	29.281(6)	14.001(2)	28.838(6)	113.087(3)	10876(4)	4

bromomethyl)pyridine by bromination with HBr and PBr_3.[7] 2, 6-Bis(amino-methyl)pyridine hydrochloride salt was reacted with the appropriate isocyanate (4-(trifluoromethyl)phenyl isocyanate, 3,5-bis(trifluoromethyl) phenyl isocyanate and 4-nitrophenyl isocyanate) under the same reaction conditions used for **L^1**, **L^3**, and **L^5** to obtain the desired compounds in 52-74% yield (see ESI† for further details).

Receptors **L^1-L^6** were crystallized by slow evaporation from various solvents (see Table S1 in the ESI†). Interestingly, only receptors **L^3** and **L^4** showed a tendency to form crystals suitable for single crystal X-ray investigation.

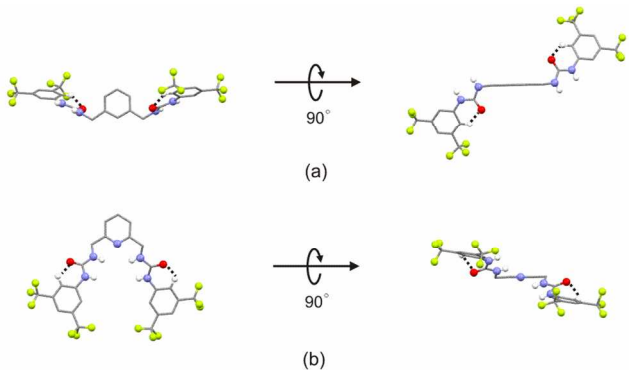

Figure 1. Molecular conformations of the three structures (a) **L^3-DMSO** (as representative of the two isostructures **L^3-DMSO** and **L^4-MeOH**) and (b) **L^4-A**. The conformations are represented along two perpendicular directions (left and right). The orientation of the molecules is chosen to best show the open and closed conformations.

Crystallization of receptors **L^3** and **L^4** by slow evaporation from saturated solutions of DMSO, resulted in the formation of a DMSO solvate for receptor **L^3** (**L^3-DMSO**) and an anhydrous form for receptor **L^4** (**L^4-A**). Interestingly, when receptor **L^4** was crystallised by slow evaporation from a saturated solution of MeOH a solvate (**L^4-MeOH**) isostructural with **L^3-DMSO** was obtained.

A summary of the basic crystallographic parameters and the crystal packing for all the structures are reported in Table 1 and Table S2 and Figure S1 in the ESI† respectively. All the structures crystallise in monoclinic crystal system (space group C2/c for the two solvates **L^3-DMSO** and **L^4-MeOH** and space group P2/c for **L^4-A**). A comparison of the two types of crystal packing shows major differences. In the two isostructures **L^3-DMSO** and **L^4-MeOH** (Figure 1a for **L^3-DMSO** as representative of the two isostructures **L^3-DMSO** and **L^4-MeOH**) the four urea N-H groups are approximately oriented perpendicular to the plane of the aromatic spacer resulting in an open conformation. However, in **L^4-A** (Figure 1b) the four urea N-H groups are oriented to form a pseudo-cavity adopting a closed folded conformation. In the three structures adjacent molecules are connected one to each other *via* N-H···O hydrogen bonds between the urea NHs of one unit and the oxygens of the carbonyl group of another unit, and related by inversion symmetry to form an infinite 1-D molecular arrangements (Figures 2a and b) which propagates along the [001] direction (for a detailed descriptions of the main intermolecular interactions involved see Table S3 in ESI).

In the two isostructures **L^3-DMSO** and **L^4-MeOH**, N-H···O distances are respectively 2.05 Å and 2.13 Å for the former and 2.04 Å and 2.07 Å for the latter. In **L^4-A** N-H···O distances are 2.25 Å and 1.99 Å respectively. In all the structures these chains are then assembled along the remaining two dimensions to

generate the 3-D packing (for a detailed representation of the crystal packing see Figure S1c). Interestingly the CF_3 groups seem to have a specific role in this, participating with the F atoms in the formation of C-H···F interactions (see Table S3 in ESI†), which, in some cases, show distances which are slightly less than the sum of the van der Waals radii of hydrogen and fluorine, (considering the value of 2.67 Å proposed by Bondi[8]).

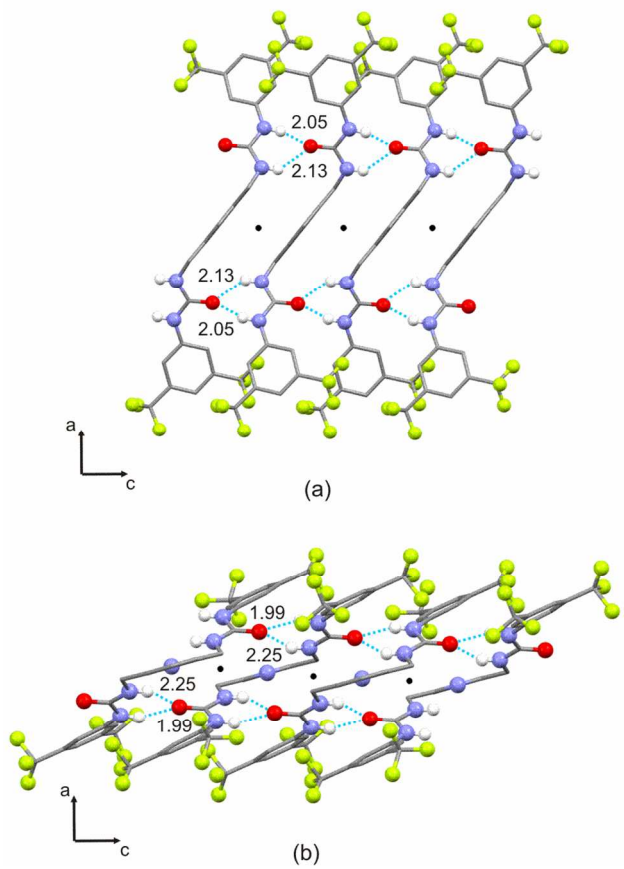

Figure 2. Portion of the 1-D crystal packing of the X-ray crystal structure of (a) compound **L³-DMSO** reported as representative of the isostructural set **L³-DMSO/L⁴-MeOH** and (b) compound **L⁴-A**. The most relevant interactions are represented as blue dashed lines (intermolecular distances are expressed in angstroms), centre of inversions are also represented as black circles.

Although there are cases in which this interaction showed a high degree of directionality, even in presence of competing groups able to form stronger interactions, [9] in this case their role in driving the assembly of specific molecular arrangement might be questionable but certainly contributes to the overall stability of the structures.

2.2. Solution anion binding studies and solid-state characterisation

The ability of compounds **L¹-L⁶** to bind anions (specifically AcO^-, BzO^-, Cl^-, F^-, HCO_3^-, $H_2PO_4^-$, and NO_3^-) in solution was investigated using ^1H NMR titration techniques in DMSO-d_6/0.5% H_2O (with the anions added as tetrabutylammonium (TBA) or tetraethylammonium (TEA) salts). Where possible the change in chemical shift of the most downfield NH signal was fitted to a 1:1 binding model using WinEQNMR software (see Figures S26-S57 in ESI† for fittings).[10] The results are summarised in Table 2. We observed that only compounds **L²** and **L⁴** demonstrated strong 1:1 binding with tetrabutylammonium fluoride (K_a >10^4 M^{-1}) and moderate 1:1 binding with tetrabutylammonium dihydrogenphosphate.

Table 2. Stability constants K_a (M^{-1}) for compounds **L¹-L⁶** with the tetrabutylammonium or tetraethylammonium salts of the anion considered in DMSO-d_6/0.5% water at 300 K. All errors estimated to be <10% (See ESI† Figs. S26-S57 for the fittings for each titration).

Anions	L¹	L²	L³	L⁴	L⁵	L⁶
AcO^-	152	342	187	357	242	657
BzO^-	124	174	180	183	172	277
$H_2PO_4^-$	582	1842	592	1730	475	2652
HCO_3^-	124	793	506	594	part depr	537
NO_3^-	no[a] inter	no[a] inter.	no[a] inter	no[a] inter	no[a] inter	no[a] inter.
F^-	depr.[b]	>10^4	depr.[b]	>10^4	depr.[b]	depr.[b]
Cl^-	32	141	35	168	44	229

[a]None of the urea protons showed significant shifts upon addition of NO_3^-; [b]We observed the broadening and subsequent disappearance of the urea NH resonances.

The other compounds had moderate affinity (or in the case of nitrate no interaction) for the anions studied.

Receptors **L¹-L⁶** were crystallised by slow evaporation from various solvents in presence of anionic guests. Details of the crystallization experiments, both successful and unsuccessful, are provided in ESI† (Table S1). Crystals suitable for single crystal X-ray investigation were only obtained for host-guest complexes involving receptors **L¹-L⁴**.

The majority of the structures (see Table S2 and Figure S1 in ESI† and Table 1) crystallise in the monoclinic crystal system with the only exception being the structure **$L^3CO_3^{2-}$ (2:1)** which adopts an orthorhombic crystal system. In the five structures, the receptor units show a wide variety of conformational choices (Figure 3).

This is consistent with the absence of any set of strong intra-molecular interactions, that are able to lock or stabilize a specific conformation.[11] The only intramolecular interactions observed is the C-H···O interaction (C-H···O distances are in the range 2.2-2.5 Å, as described in Table S3 in ESI) involving the aromatic C-H and the urea C=O (Figure 1 a-b and Figure 3 a-e) which force the urea group and the aromatic substituted ring of the target receptors to lie in the same plane. However, similarly to that we

observed for the crystal structures of the free

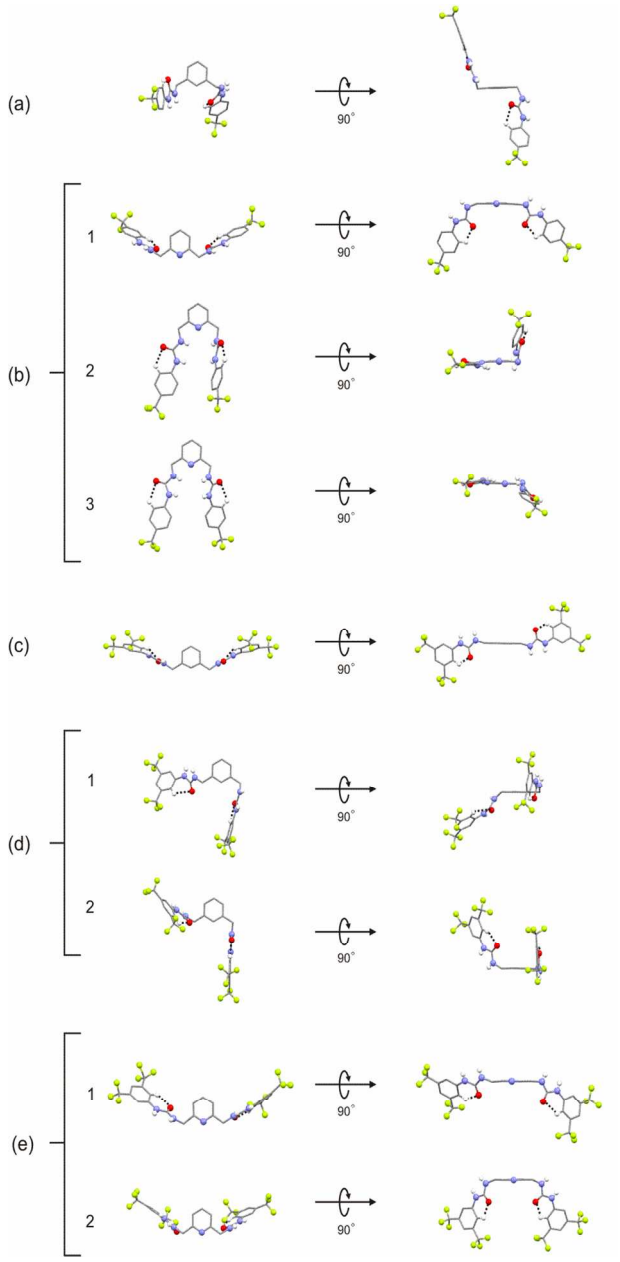

Figure 3. Molecular conformations of the three structures (a) **L^1-AcO^- (1:2)** (open); (b) symmetrically independent molecule 1 (open), 2 (closed) and 3 (closed) for the structure **L^2-SO_4^{2-}(3:1)**; (c) **L^3-AcO^-(1:2)** (open); (d) symmetrically independent molecule 1 (open) and 2 (open) for the structure **L^3-CO_3^{2-}(2:1)**; (e) symmetrically independent molecule 1 (open) and 2 (open) for the structure **L^4-HPO_4^{2-}(2:1)**. The conformations are represented along two perpendicular directions (left and right). The orientation of the molecules is chosen to best show the open and closed conformations.

receptors (**L^3-DMSO**, **L^4-A** and **L^4-MeOH**), we can outline two basic behaviours, open and closed, simply by considering the reciprocal orientation of the ureidic NH groups. It is interesting to note that the majority of the structures adopt the open conformation (see Figures 3 a, b1, c, d, e), with the urea NHs externally exposed and available for interactions with the anions, favouring host–guest stoichiometry higher than 1:1. This is in contrast with the behaviours observed in solution where stoichiometries 1:1 were obtained. However this result is not surprising considering that the stability of the stoichiometry adopted by a binary complex might depends on several factors such as the concentration and the solvent used.[12]

In this regard, also the molecular features of the anionic guest involved, might play a role. The combination of different parameters, such as the number of hydrogen bond acceptors and the resulting shape of the anionic species together with the directionality of the intermolecular interactions involved might favour one specific stoichiometry rather than another. For example, in the case of carboxylate anions, the urea NHs can efficiently interact with the two acceptor oxygens *via* N-H···O hydrogen bond interactions with N-H···O angles at approximately 180 degrees. This would favour 1:1 urea-carboxylate ratios. In the case of the other anionic species reported here (**SO_4^{2-}**, **CO_3^{2-}**, **HPO_4^{2-}**), the increased number of the hydrogen bond acceptor oxygens, together with the directionality of the interactions, can promote interactions with more than one receptor unit, enabling higher stoichiometries (2:1 and /or 3:1). Starting from these considerations we decided to discuss the structures separately, depending on the stoichiometry observed (1:2, 2:1 and 3:1).

1:2 ratio

According to the considerations reported above, the two acetates **L^1-AcO^-(1:2)** and **L^3-AcO^-(1:2)** adopt a urea/carboxylate 1:1 ratio, resulting in a overall 1:2 stoichiometry.

Single crystals of **L^1-AcO^-(1:2)** were obtained by slow evaporation from a solution of the receptor **L^1** in THF/DMF 9:1 and in presence of an excess of TBA^+AcO^-.

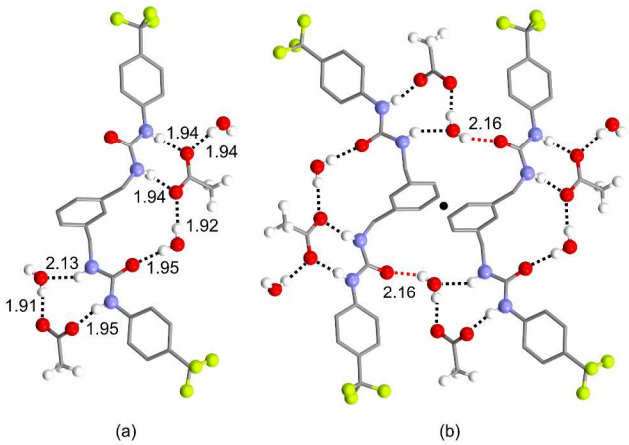

Figure 4. Main receptor-anion interactions in structure **L^1-AcO^-(1:2).** a) Monomeric arrangement; b) centrosymmetric dimeric arrangement. Intermolecular interactions are represented as black dashed lines. Intermolecular interactions between two monomeric units are indicated as red dashed lines, centre of inversions are also represented as black circles.

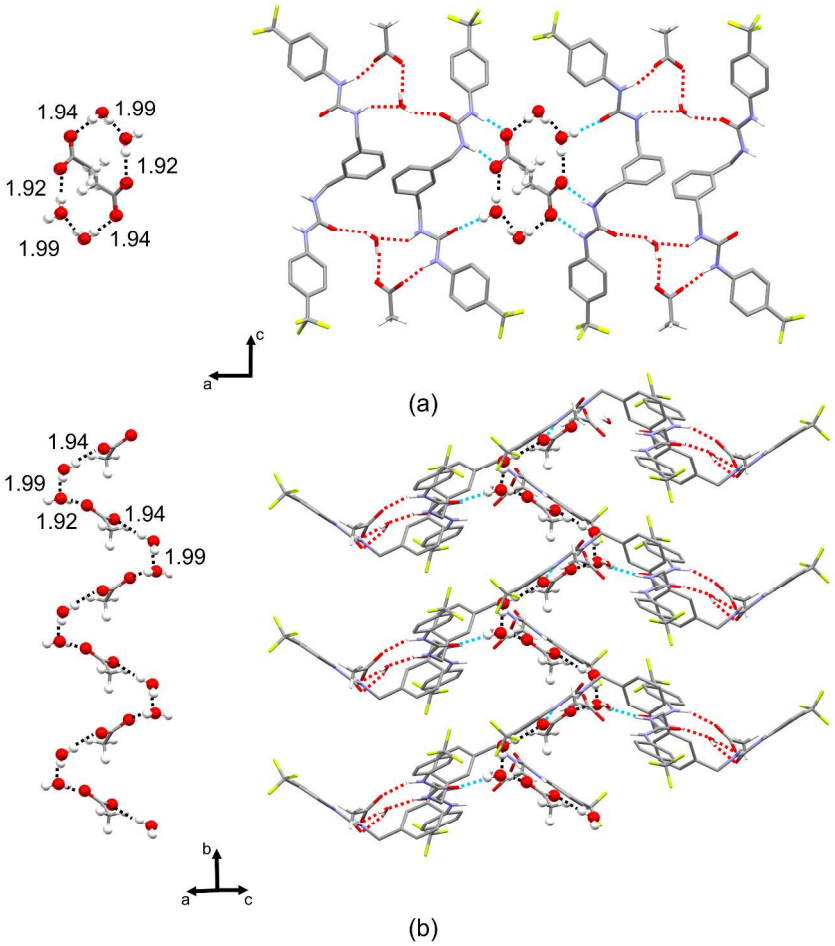

Figure 5 Water-acetate infinite helices and their role in driving molecular arrangements viewed along the [010] direction (a) and along the [101] direction (b). Intermolecular interactions are colour coded depending on their role: black dashed lines are used for interactions involved in the formation of the helices, blue dashed lines for helices-receptors interactions, red dashed lines for receptor-receptor interactions.

The complex crystallizes in the monoclinic crystal system (space group *I2/a*;). The asymmetric unit of **L^1-AcO$^-$(1:2)** contains one receptor unit (**L^1**), two TBA^+AcO^- and three H_2O molecules. The acetate anions are connected to the receptor unit *via* N-H···O interactions involving the carboxylate oxygens and the urea NHs (see Table S3 in ESI). Interestingly only one of the two urea sites show the typical carboxylate-urea geometry, with the urea-carboxylate groups lying in the same plane (Figure 4 a) and connected *via* two N-H···O hydrogen bonds (N-H···O distances are for both interactions 1.94 Å). In the other binding site the second acetate only interacts *via* one N-H···O interaction (N-H···O distance is 1.95 Å) and the typical geometry is distorted by the presence of one water molecule (Figure 4a) which replaces one of the urea-carboxylate N-H···O interactions with a N-H···O-H···O bridge (N-H···O_w and O-H_w···O distances are 2.13 Å and 1.91 Å respectively). This is not uncommon, [13, 14] and often hydrates and, generally, solvates might influence the expected geometry for a given pair of interacting functional groups.

The same water molecule is also involved in O-H···O hydrogen bond (O-H_w···O distances is 2.16 Å) with the urea C=O of an adjacent molecule forming a centrosymmetric dimer (red dashed line in Figure 4 b). The remaining two water molecules are involved in the formation of an $AcO^-···H_2O···H_2O···AcO^-$ infinite helices (O-H_w···O_{AcO} distances are 1.92 Å and 1.94 Årespectively, O-H_w···O_w distance is 1.99 Å) spiraling around the [010] direction under the effect of the 2_1 screw axis (Figures 5 a and b left).

This arrangement bridges adjacent dimers along the helices *via* the coplanar urea/carboxylate interaction described above, resulting in a propagation of the centrosymmetric dimers along both, the [100] and the [010] direction (Figures 5 a and b right). The centrosymmetric dimers are then assembled along the remaining direction, [001], by weak C-H···F contacts (C-H···F distance is 2.74 Å). The TBA^+ cations, omitted from Figures 4 and 5 for clarity, do not show any particular role in driving specific molecular arrangements and are connected to receptor

molecules *via* a set of C-H···O and C-H···F contacts. Details of the 3-D packing are shown in Figure S1d in ESI†.

Despite the similar molecular structure and the presence of the same anionic guest, the crystal structure of **L^3-AcO$^-$(1:2)** shows major departures with respect to the structure discussed

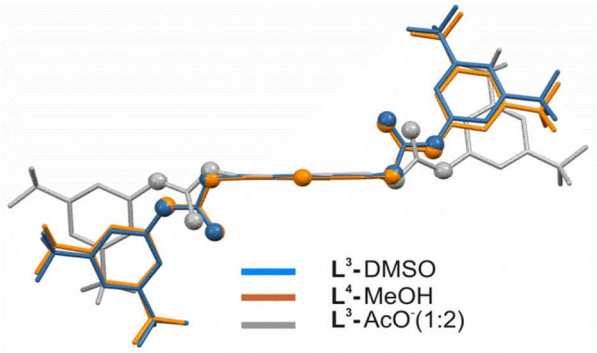

Figure 6. Differences in the open conformation for the three structures **L^3-DMSO** (blue), **L^4-MeOH** (orange) and **L^3-AcO-(1:2)** (grey).

previously **L^1-AcO$^-$(1:2)**. **L^3-AcO$^-$(1:2)** was crystallised by slow evaporation from a solution in EtOH/$MeNO_2$ (1:1) of the receptor **L^3** in presence of an excess of TBA^+AcO^-. The sample crystallised in the monoclinic crystal system (space group I2/a). The crystal structure contains one receptor unit and two TBA^+AcO^- units. It is interesting to note that similarly to the two isostructures **L^3-DMSO** and **L^4-MeOH**, **L^3-AcO$^-$(1:2)** adopts an open conformation with the urea NHs oriented to opposite directions and perpendicular to the aromatic spacer. A conformational comparison of the three molecules is shown in Figure 6.

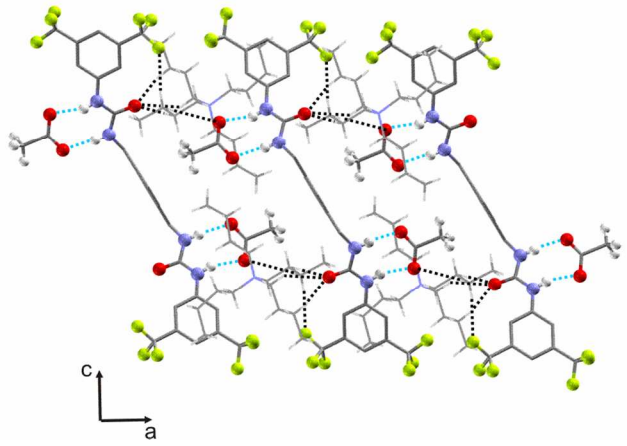

Figure 7. Portion of the 1-D crystal packing of the X-ray crystal structure **L^3-AcO-(1:2).** N-H···O hydrogen bonds are represented as blue dashed lines, C-H···F and C-H···O interactions as black dashed lines

Each receptor unit is connected to two AcO^- anions *via* N-H···O hydrogen bonds (N-H···O distances are 1.99 Å and 1.90 Å respectively) and related to adjacent molecules by inversion symmetry (see Table S3 in ESI). These are bridged by TBA^+ cations *via* a set of weak C-H···O hydrogen bonds (the shortest C-H···O distances observed is 2.42 Å) involving the urea C=O and the acetate oxygens and a C-H···F interaction (C-H···F distance is 2.57 Å), resulting in a 1-D arrangement along the [100] direction (Figure 7).

Similar bridges are also observed in the remaining two dimensions, where TBA^+ cations connect different receptor-anions units *via* a set of weak C-H···O and C-H···F interactions (see Figure S1e in ESI).

It is interesting to note that, differently to the previous acetate structure, where the presence of water molecules strongly contributed in driving the crystal packing, here the TBA^+ cations have a specific role in connecting the receptor-anion units along the different directions of the packing. A detailed representation of the 3-D crystal packing is reported in Figure S1e in ESI.†

2:1 ratio

This specific stoichiometry was observed for the two structures **L^3-CO_3^{2-} (2:1)** and **L^4-HPO_4^{2-}(2:1)**. Differently to the previous structures, the molecular features of the anionic guests and the increased stoichiometry of the two host-guest pairs result in a more complex crystal packing. In contrast to the approach taken so far to describe the crystal structures, in this case and for the 3:1 stoichiometry, it is more convenient to focus on the coordination of the anionic moieties and consider these as building units of particular molecular arrangements. This is consistent with the recently proposed analogies between transition-metal coordination chemistry[15] and anion binding. In order to determine the number of hydrogen bonds involved in anion binding, we decided to apply in this case a starting limit of 2.75 Å to identify N-H···O hydrogen bonds and, where relevant, to take into account slightly longer interactions.

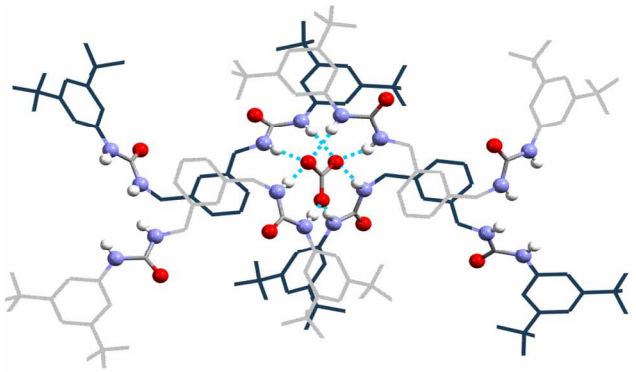

Figure 8. Receptor-anion coordination In structure **L^3-CO_3^{2-} (2:1).** The two independent receptor units, 1 and 2, are coloured in grey and blue respectively. Intermolecular interactions involved in the coordination of the CO_3^{2-} anion are indicated as blue dashed lines.

Cite this: DOI: 10.1039/c0xx00000x

www.rsc.org/xxxxxx

ARTICLE TYPE

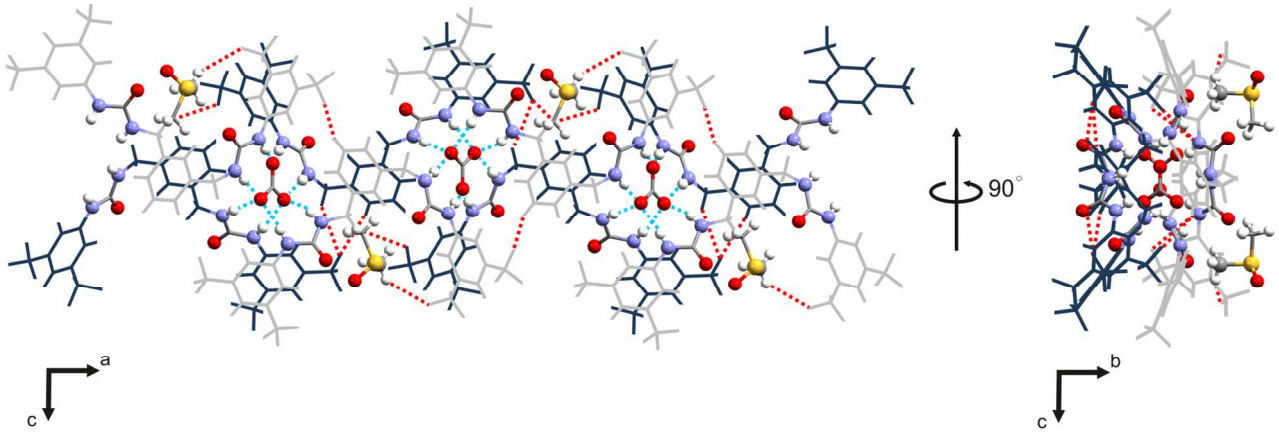

Figure 9. Portion of the 1-D crystal packing of the X-ray crystal structure **L^3-CO_3^{2-} (2:1)** viewed along the [010] direction (left) and along the [100] direction (right). Anion-receptor interactions are represented as blue dashed lines, C-H···F intermolecular interactions as red dashed lines. The two independent receptor units, 1 and 2, are coloured in grey and blue respectively. Solvent molecules (DMSO) are also shown.

Slow evaporation of a DMSO solution of the receptor in the presence of an excess of tetrabutylammonium cyanide afforded crystals of **L^3-CO_3^{2-} (2:1)** as colourless needles. The presence of the CO_3^{2-} might originate from CO_2 in the atmosphere that has presumably been fixed by the receptor-cyanide solution. Analogous carbon dioxide fixation in the presence of basic tetrabutylammonium salts have been previously reported, [16-19] however this appears to be the first case in the presence of TBA^+CN^-. The resulting crystal structure adopts the orthorhombic crystal system (space group Pbca), with an asymmetric unit containing two independent receptor units, two molecules of DMSO and one CO_3^{2-} with two TBA^+ as counterions. Each CO_3^{2-} anion is tetra-coordinated by four receptor units, (two per each independent units 1 and 2) *via* eight N-H···O hydrogen bonds (N-H···O distances are in the range 1.88 - 2.06 Å), each interacting with one of the two urea groups available, resulting in a 2:1 stoichiometry (Figure 8). The remaining urea groups are connected to adjacent receptor units by CO_3^{2-} bridges, to form infinite chains propagating along the [100] direction (Figure 9). These are also assisted by weak C-H···F interactions involving the terminal CF_3 groups and the aromatic CHs (C-H···F distances are 2.49 Å and 2.99 Å respectively).

Similarly to the previous structure, the TBA^+ units are strongly involved in connecting the receptor-anion units along the different directions of the packing. In contrast to the hydrate structure **L^1-AcO^- (1:2)**, described earlier, the solvent (DMSO) does not seem to have any specific role in directing particular molecular arrangements. However, it takes part with TBA^+ units, in connecting adjacent 1-D chains along [010] and [001] directions *via* different sets of C-H···O and C-H···F interactions (the shortest C-H···O and C-H···F distances observed are 2.22 Å and 2.08 Å respectively). A detailed representation of the 3-D crystal packing and all the intermolecular interactions involved are reported in Figure S1f and table S3 in ESI†.

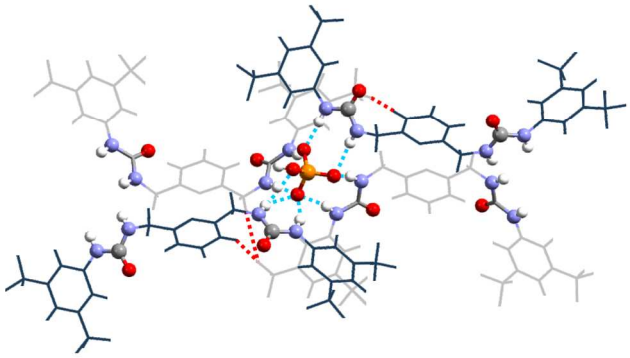

Figure 10. Receptor-anion coordination in structure **L^4-HPO_4^{2-}(2:1).** The two independent receptor units, 1 and 2, are coloured in grey and blue respectively. Intermolecular interactions involved in the coordination of the HPO_4^{2-} anion are indicated as blue dashed lines. The arrangement is oriented to best show the receptor-anion coordination.

L^4-HPO_4^{2-}(2:1) was crystallised by slow evaporation from a DMSO solution of the receptor **L^4** in the presence of an excess of $TBA^+H_2PO_4^-$. Interestingly the oxo-anion deprotonates in the solid-state structure. This deprotonation process has been observed previously upon crystallisation of protonated oxo-anions with receptors containing multiple hydrogen bond donors.[20, 21] The structure adopts a monoclinic crystal system (space group

Cite this: DOI: 10.1039/c0xx00000x

www.rsc.org/xxxxxx

ARTICLE TYPE

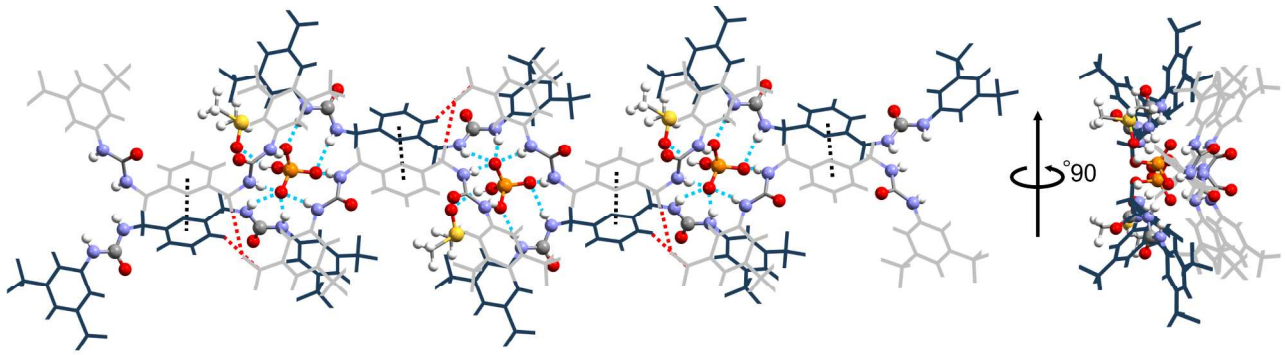

Figure 11. Portion of the 1-D crystal packing of the X-ray crystal structure **L^4-HPO_4^{2-}(2:1)** propagating along the [101] direction, showed along two perpendicular directions. Anion-receptor interactions are represented as blue dashed lines, C-H···F intermolecular interactions as red dashed lines and π···π stacking as black dashed lines. The two independent receptor units, 1 and 2, are coloured in grey and blue respectively. Solvent molecules (DMSO) are also shown.

$P2_1/n$) with two independent receptor units, two TBA^+, one HPO_4^- and one molecule of DMSO in the asymmetric unit. Each HPO_4^- unit is surrounded by four receptor units (two per each independent unit 1 and 2), interacting with only one of the two urea groups available (Figure 10), *via* nine N-H···O hydrogen bonds (N-H···O distances lie in the range 1.87 - 2.62 Å, see Table S3 in ESI†). The remaining urea groups interact, as also observed in **L^3-CO_3^{2-} (2:1)**, with adjacent HPO_4^- units to form an infinite 1-D chain propagating along the [101] direction (Figure 11). It is interesting to note in this structure the contribution of weak contacts, such as π···π stacking (cen-cen distance for the two aromatic spacers is 3.64 Å) and C-H···F (C-H···F distances are 2.70 Å and 2.77 Å), in connecting the different units within the 1-D arrangement (Figure 11).

Similarly to **L^3-CO_3^{2-} (2:1)** the solvent molecules (DMSO) does not actively partecipate in driving any relevant molecular arrangement but it simply bridges adjacent 1-D chains along the [010] direction *via* C-H···F, O-H···O and C-H···O interactions (C-H···F and O-H···O distances are 2.65 Å and 1.89 Å respectively; C-H···O are 2.74 Å). A similar contribution is also given by the TBA^+ units, which bridge, *via* a set of weak C-H···F interactions, adjacent 1-D chains along the remaining two dimension of the packing (for a detailed representation of the crystal packing see Figure S1g in ESI†).

3:1 ratio

L^2-SO_4^{2-}(3:1) was crystallised by slow evaporation from a DMSO solution of the receptor **L^2** in presence of an excess of $TBA^+HSO_4^-$.

The structure adopts a monoclinic crystal system (space group $P2_1/c$) with an asymmetric unit containing three receptor units, one SO_4^{2-}, two TBA^+ units and two H_2O molecules.

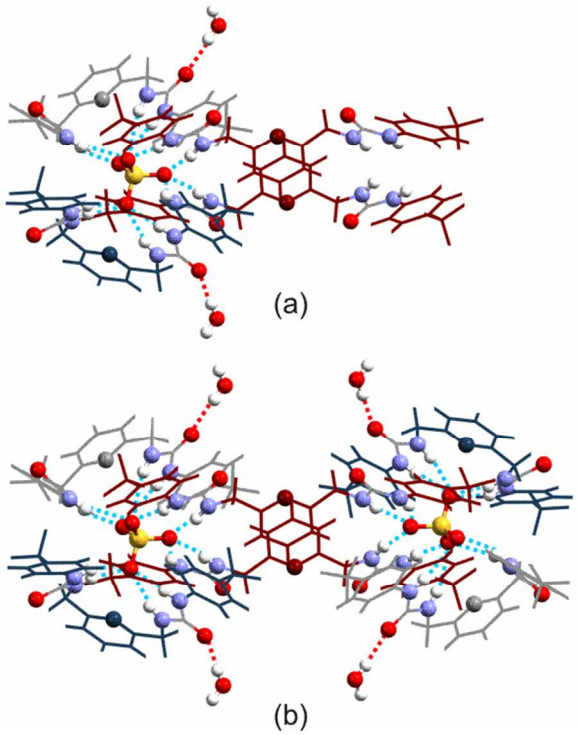

Figure 12. Receptor-anion coordination in structure **L^2-SO_4^{2-}(3:1)** viewed along the [001] direction. a) coordination of one SO_4^{2-} anion; b) dimeric arrangement with two SO_4^{2-} anions coordinated by receptors 1, 2 and 3. The three independent receptor units, 1, 2 and 3 are coloured in red, grey and blue respectively. Intermolecular interactions involved in the coordination of the SO_4^{2-} anion are indicated as blue dashed lines, O-H···O hydrogen bonds as red dashed lines. Water molecules are also shown.

In contrast to the previous receptor-anion complexes, which mainly adopt an open conformation, in **L^2-SO_4^{2-}(3:1)** two of the three independent receptor units (2 and 3) adopt a closed conformation, with the urea NHs oriented to form a pseudo-cavity.

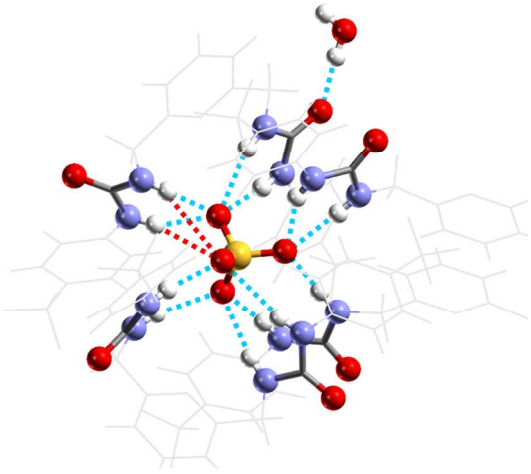

Figure 13. Receptor-anion coordination in structure **L^2-SO_4^{2-}(3:1)** oriented to best show the twelve N-H···O hydrogen bonds (blue dashed lines). Hydrogen bonds above the 2.75 Å cut-off (red dashed lines) are also shown. Urea groups are highlighted for clarity. Water molecules are also shown.

These both coordinate the SO_4^{2-} *via* eight N-H···O hydrogen bonds (receptor blue and grey in Figure 12 a). The coordination is completed by two independent receptors 1 (red in Figure 12 a) that adopt an open conformation and contribute to the coordination with only one of the available urea groups.

This results in a 3:1 stoichiometry with the SO_4^{2-} anion surrounded by four receptor units: two of the type 1 and one of the type 2 and 3 (Figure 12 a) and connected *via* a total of twelve[21] N-H···O hydrogen bonds (N-H···O hydrogen bonds are in the range 1.99-2.49 Å, see Table S3 in ESI†). This, according to previous papers by Custelcean *et al* [23,24] represents the optimal coordination number for sulfate. An instance of the coordination of the SO_4^{2-} anion is shown in Figure 13, where the urea groups are highlighted for clarity. This cluster is connected to a second SO_4^{2-} *via* the available urea groups of receptor 1 to form a sort of dimeric arrangement (Figure 12 b).This is connected to adjacent dimers *via* different sets of intermolecular interactions, including O-H···O, C-H···F and C-H···O. In particular C-H···F interactions (C-H···F distance is 2.77 Å) operate along the [100] direction, connecting different instances of the dimer to form a 1-D chain in which adjacent components are related by inversion symmetry (Figure 14).

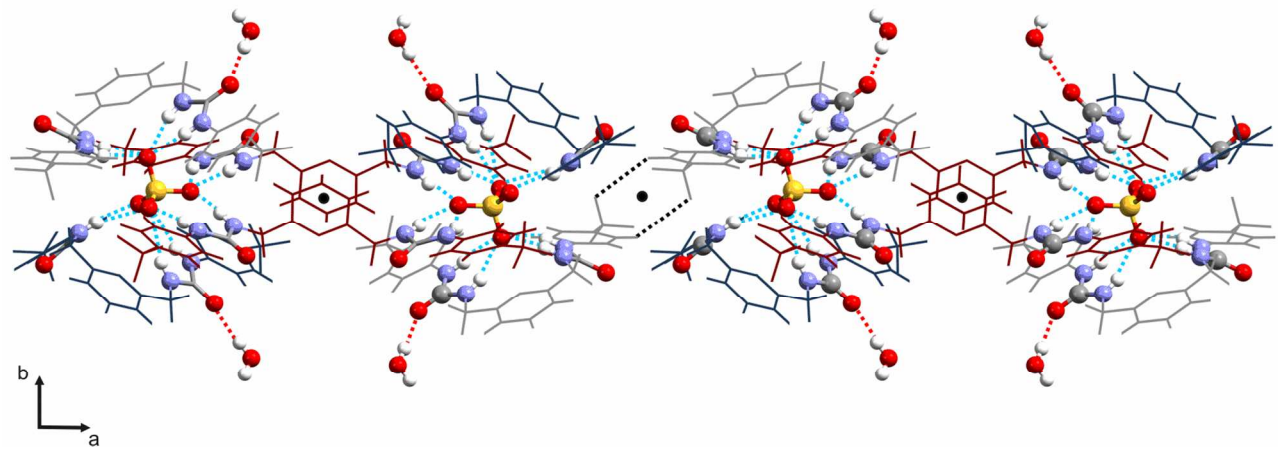

Figure 14. Portion of the 1-D crystal packing of the X-ray crystal structure **L^2-SO_4^{2-}(3:1)** viewed along the [001] direction showing propagation of the dimeric cluster along the [100] direction. Anion-receptor interactions are represented as blue dashed lines, C-H···F intermolecular interactions as black dashed lines, O-H···O hydrogen bonds as red dashed lines. The three independent receptor units, 1, 2 and 3 are coloured in red, grey and blue respectively. Water molecules are also reported. Centre of inversions are represented as black circles.

This inversion symmetry is also observed along the [010] direction where adjacent dimers are bridged by water molecules (Figure 15) *via* strong O-H···O hydrogen bonds (O-H···O distances are 1.76 Å and 2.15 Å respectively).

It is interesting to note, again, the important role of water in driving specific molecular arrangements, as already seen for **L^1-AcO$^-$(1:2)**. This arises from its intrinsic features such as its small size and the simultaneous presence of hydrogen bond donors and acceptors which make water suitable for bridging different molecules. Similarly to the previous structures it is worth highlighting the role of C-H···F interactions (C-H···F distances are in the range 2.55-2.99 Å) which are responsible for the propagation of the dimeric cluster along the remaining direction of the crystal packing [001]. A more detailed representation of the crystal packing is reported in Figure S1h in ESI†.

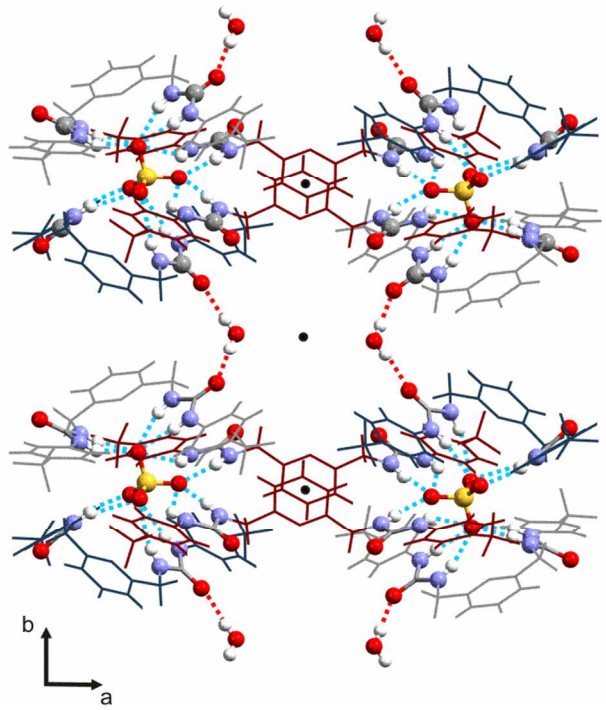

Figure 15. Portion of the 1-D crystal packing of the X-ray crystal structure **L^2-SO_4^{2-}(3:1)** viewed along the [001] direction showing propagation of the dimeric cluster along the [010] direction. Anion-receptor interactions are represented as blue dashed lines, C-H···F intermolecular interactions as black dashed lines, O-H···O hydrogen bonds as red dashed lines. The three independent receptor units, 1, 2 and 3 are coloured in red, grey and blue respectively. Water molecules are also represented. Centre of inversions are represented as black circles.

Anion transport studies in lipid bilayers

The anion transport properties of receptors **L^1-L^6** were studied using vesicle-based methods.[25] A sample of unilamellar POPC vesicles was prepared containing 489 mM NaCl buffered to pH 7.2 with 5 mM sodium phosphate salts. The vesicles were suspended at a lipid concentration of 1 mM in 489 mM $NaNO_3$ buffered to pH 7.2 with 5 mM sodium phosphate salts. The experiment was initiated by the addition of a small amount of a DMSO solution of the receptor (0.02-2 mol% with respect to lipid), and the resulting chloride efflux was monitored using a chloride ion selective electrode (ISE). At the end of the experiment (300 s), the vesicles were lysed by addition of detergent, and the final electrode reading was used to calibrate 100% chloride release. We found that all the compounds except **L^1** (i.e. L^2-L^6) were capable of mediating chloride transport under these conditions (Figure 16 and Figures S3-S11 in ESI†). For this reason all the following studies were performed on **L^2-L^6**. In order to determine the mechanism of chloride release by receptors **L^2-L^6** we performed a second experiment using POPC vesicles containing 450 mM NaCl buffered to pH 7.2 with 20 mM sodium phosphate salts.

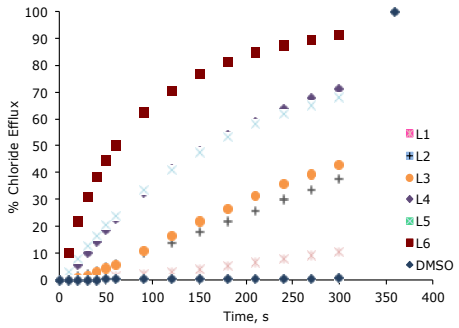

Figure 16. Chloride efflux promoted by a DMSO solution of **L^1-L^6** (2 mol% carrier to lipid) from unilamellar POPC vesicles loaded with 489 mM NaCl buffered to pH 7.2 with 5 mM sodium phosphate salts. The vesicles were dispersed in 489 mM $NaNO_3$ buffered to pH 7.2 with 5 mM sodium phosphate salts. At the end of the experiment detergent was added to lyse the vesicles and calibrate the ISE to 100% chloride efflux. Each point represents an average of three trials. DMSO was used as a control.

The vesicles were suspended in 162 mM Na_2SO_4 buffered to pH 7.2 with 20 mM sodium phosphate salts. Upon addition of a transporter **L^2-L^6** in a solution of DMSO at 2 mol% with respect to lipid, there was negligible chloride release. This indicates that these receptors function predominantly by an anion exchange mechanism. In the first assay, the receptors were shown to facilitate Cl^-/NO_3^- exchange, however in the second assay, little transport was observed due to the high hydrophilicity of the SO_4^{2-} anion,[26] which usually prevents its transport by synthetic transporters.[27] After 120 s, a pulse of $NaHCO_3$ solution was added, and we observed that the receptors (except **L^2**) were able to begin mediating chloride efflux (Figure 17 and Figures S13-S19 in ESI†), evidence in support of Cl^-/HCO_3^- antiport mechanism although the compounds proved to be less active for chloride/bicarbonate exchange than for chloride/nitrate antiport. The lack of transport in the absence of a readily transportable external anion was not perturbed by changing the encapsulated cation, thus implying that a M^+/Cl^- co-

transport mechanism is not possible (see Figure S21 in ESI†).

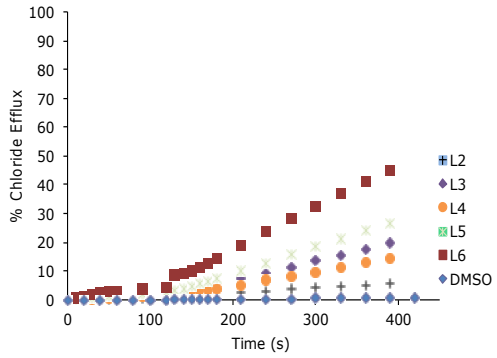

Figure 17 Chloride efflux promoted by a DMSO solution of compounds L^2–L^6 (2 mol% carrier to lipid) from unilamellar POPC vesicles loaded with 451 mM NaCl buffered to pH 7.2 with 20 mM sodium phosphate salts. The vesicles were dispersed in 150 mM Na_2SO_4 buffered to pH 7.2 with 20 mM sodium phosphate salts. At 120 s a solution of sodium bicarbonate was added such that the external concentration of bicarbonate was 40 mM. At the end of the experiment, detergent was added to lyse the vesicles and calibrate the ISE to 100% chloride efflux. Each point represents an average of three trials. DMSO was used as a control.

In order to gather further evidence for a mobile carrier mechanism, we tested the Cl^-/NO_3^- antiport activity of L^2-L^6 in vesicles composed of POPC/cholesterol (7:3). The presence of cholesterol results in ordering of the bilayer, increasing its viscosity resulting in a slowing of the diffusion of a mobile carrier. Compounds L^2-L^6 showed a reduced rate of transport in the POPC/cholesterol system (see Figures S22-S25 in ESI† for L^2-L^5), evidence consistent with a mobile carrier mechanism.[28] In Figure 18, the chloride efflux mediated by L^6 in POPC or POPC/cholesterol (7:3 molar ratio) is shown as an example.

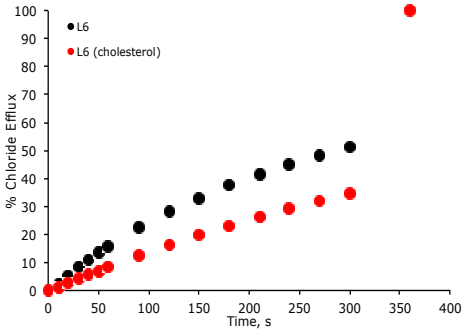

Figure 18. Chloride efflux promoted by a DMSO solution of compound L^6 (0.2mol% carrier to lipid) from unilamellar vesicles comprising of either POPC or POPC/cholesterol (7:3 molar ratio), loaded with 489mM NaCl buffered to pH 7.2 with 5mM sodium phosphate salts. The vesicles were dispersed in 489mM $NaNO_3$ buffered to pH 7.2 with 5mM sodium phosphate salts. At the end of the experiment detergent was added to lyse the vesicles and calibrate the ISE to 100% chloride efflux. Each point represents an average of three trials. DMSO was used as a control.

To quantify the transport activity of compounds L^2–L^6 Hill analyses[29] for the chloride/nitrate and chloride/bicarbonate antiport assays were performed (see Figures S4-S20 in ESI†).

Table 3. The EC_{50} is the concentration (mol% carrier to lipid) needed to obtain 50% efflux after 270s and n is the Hill coefficient that represents an estimate of the number of transporter molecules required to transport a single anion.

Compound	$EC_{50,270s}$ (Cl^-/NO_3^-)	n	$EC_{50,270s}$ (Cl^-/HCO_3^-)	n
L^2	3.6	1.2	--	--
L^3	2.8	1.6	7.9	0.9
L^4	1.3	1.1	10.7	1
L^5	1.0	0.9	6.8	0.8
L^6	0.2	1.1	2.3	0.8

Hill analysis enables the $EC_{50,270s}$ value to be obtained, which is a measure of transporter efficiency, defined as the required receptor concentration to mediate 50% of the total chloride efflux 270s after the addition of the carrier (or after the bicarbonate 'pulse').

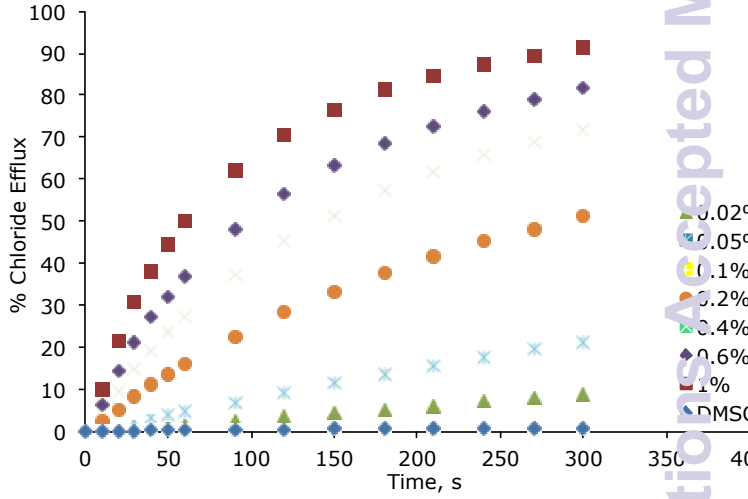

(a)

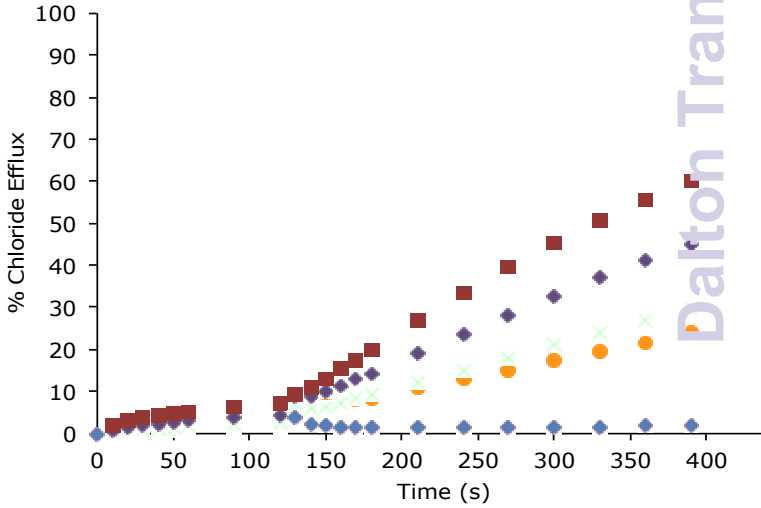

(b)

Figure 19. (a) Chloride efflux promoted by various concentrations of L^6 from unilamellar POPC vesicles loaded with 489 mM NaCl buffered to pH 7.2 with 5 mM sodium phosphate salts. The vesicles were dispersed in

489 mM $NaNO_3$ buffered to pH 7.2 with 5 mM sodium phosphate salts.; (b) Chloride efflux promoted by various concentrations of **L**^{6} from unilamellar POPC vesicles loaded with 451 mM NaCl buffered to pH 7.2 with 20 mM sodium phosphate salts. The vesicles were dispersed in 150 mM Na_2SO_4 buffered to pH 7.2 with 20 mM sodium phosphate salts. At 120 s a solution of sodium bicarbonate was added such that the external concentration of bicarbonate was 40 mM. At the end of both experiments, detergent was added to lyse the vesicles and calibrate the ISE to 100% chloride efflux. In both graphs each point represents an average of three trials. DMSO was used as a control.

This allows us to compare the transport activity of the compounds. These values are summarised in Table 3, together with the Hill coefficients, which are commonly interpreted as an estimate of the number of transporter molecules required to transport a single anion and can provide supporting evidence for a mobile carrier mechanism.

It is interesting to note that the transporter activity can be related to the electron withdrawing properties of the substituents in the pendant arms of the receptors, and to the presence of the pyridine moiety as a spacer. Indeed, the most active transporter among the series, as shown by the $EC_{50,270s}$ values of both the experiments, is the *p*-nitro functionalised compound **L**^{6} which contains a pyridine spacer (Figure 19).

Conclusions

In conclusion we have reported the synthesis of a new family of bis-methylureas (**L**^{1}-**L**^{6}), their anion binding properties (both in solution and in the solid state) and their application as anion transporters. The solid state study highlighted the high degree of flexibility of this family of receptors. The presence of four hydrogen bond donor groups on the receptors and the possibility to assume different conformations allowed the isolation in the solid state of anion-receptor adducts of different stoichiometry and the possibility to stabilise the anions with a high number of hydrogen bonds. Moreover, the new receptors are also able to work as mobile carriers for Cl^- transport through membranes with compound **L**^{6} being the most active of the series.

Acknowledgements

CC would like to thank Regione Autonoma della Sardegna (CRP-59699) for funding and for Master and Back scholarship (RM). PAG thanks the EPSRC for a DTG studentship (LEK) and the Royal Society and the Wolfson Foundation for a Royal Society Wolfson Research Merit Award. The authors thank EPSRC for funding the UK National Crystallography Service and Diamond Light Source for the use of beamline I19 under proposal MT8521.

Notes and references

[a] Dipartimento di Scienze Chimiche e Geologiche, Università degli Studi di Cagliari, S.S. 554 Bivio per Sestu, 09042, Monserrato CA, Italy. E-mail: ccaltagirone@unica.it; Tel. +39(0)70 675 4452.

[b] Chemistry, University of Southampton, Southampton, SO17 1BJ, UK. E-mail: philip.gale@soton.ac.uk; Tel: +44 (0)23 8059 3332.

† Electronic Supplementary Information (ESI) available: [Experimental methods and materials, synthesis of **L**^{1}-**L**^{6}, single crystal X-ray diffraction details (general procedures for data collection are also reported in ref 30), additional details of the anion transport studies, fittings of ^{1}H-NMR titrations.]. See DOI: 10.1039/b000000x/

1 S. Nishizawa, P. Bühlmsnn, M. Iwaho and Y. Umezawa, *Tetrahedron. Lett.*, 1995, **36**, 6483.
2 S. Nishizawa, P. Bühlmsnn, M., K.P. Xiao and Y. Umezawa, *Anal. Chim. Acta*, 1998, **358**, 35.
3 M. Emgenbroich, C. Borrelli, S. Shinde, I. Lazraq, F. Vilela, A.J. Hall, J. Oxelbark, E. De Lorenzi, J. Courtois, A. Simenova, J. Verhage, K. Irgum, K. Karim and B. Sellergren, *Chem.-Eur. J.*, 2008, **14**, 9516.
4 C. Caltagirone, C. Bazzicalupi, F. Isaia, M.E. Light, V. Lippolis, R. Montis, S. Murgia, M. Olivari, and G. Picci, *Org. Biomol. Chem.*, 2013, **11**, 2445.
5 S. J. Moore, C. J. E. Haynes, J. González, J. L. Sutton, S. J. Brooks, M. E. Light, J. Herniman, G. J. Langley, V. Soto-Cerrato, R. Pérez-Tomás, I. Marques, P. J. Costa, Vítor Félix, and Philip A. Gale, *Chem. Sci.*, 2013, **4**, 103.
6 N. Busschaert, M. Wenzel, M. E. Light, P. Iglesias-Hernández, R. Pérez-Tomás, and P. A. Gale, *J. Am. Chem. Soc.*, 2011, **133**, 14136.
7 C. Nolan and T. Gunnlaugsson, *Tetrahedron Lett.*, 2008 **49**, 1993.
8 A. Bondi, *J. Phys. Chem.* 1964, *68*, 441−451.
9 P. Panini and D. Chopra, *Cryst. Growth Des*., 2014, 14, 3155.
10 M.J. Hynes*, J. Chem. Soc., Dalton Trans.*, 1993, 311.
11 M. Olivari, C. Caltagirone, A. Garau, F. Isaia, M. E. Light, V. Lippolis, R. Montis and M. A. Scorciapino, *New J. Chem.*, 2013,**37**, 663.
12 T. Leyssens, G. Springuel, R. Montis, N. Candoni, and S. Veesler, *Cryst. Growth Des*., 2012, **12**, 1520.
13 R. Montis and M. B. Hursthouse, *CrystEngComm*, 2012, **14**, 5242.
14 R. Montis and M. B. Hursthouse, *CrystEngComm*, 2012, **14**, 7466.
15 K. Bowman-James, *Acc. Chem. Res*, 2005, **38**, 671-678.
16 T. Gunnlaugsson, P. E. Kruger, P. Jensen, F. M. Pfeffer and G. M. Husse, *Tetrahedron Lett.* 2003, **44**, 8909.
17 S. J. Brooks, P. A. Gale and M. E. Light, *Chem. Commun*., 2006, 4344.
18 S. K. Dey, R. Chutia, and G. Das, *Inorg. Chem.* 2012, **51**, 1727.
19 I. Ravikumar and P. Ghosh, *Chem. Commun.* 2010, **46**, 1082.
20 P.A. Gale, J.R. Hiscock, S.J. Moore, C. Caltagirone, M.B. Hursthouse and M.E. Light, *Chem. Asian J.,* 2010, **5**, 555.
21 N. Busschaert, P.A. Gale, C.J.E. Haynes, M.E. Light, S.J. Moore, C.C. Tong, J.T. Davis and W.A. Harrell Jr., *Chem. Commun.* 2010, **46**, 6252.

22 This number refers to N-H···O distances below the 2.75 Å cut-off. However, if we consider a less restricted definition the coordination number of SO_4^{2-} increases to 14 (there are at least other two weak hydrogen bonds, respectively at 2.81 and 2.93 Å and not included in Fig 13 but reported in Table S3 in ESI†.).
23 R. Custelcean, B. A. Moyer, B. P. Hay, *Chem. Commun.* 2005, 5971.
24 A. Rajbanshi, B. A. Moyer, R. Custelcean, *Cryst. Growth Des,* 2011, **11**, 2702.
25 B. D. Smith and T. N. Lambert, *Chem. Commun.*, 2003, 2261.
26 Y. Marcus, *J. Chem. Soc., Faraday Trans.*, 1991, **87**, 2995.
27 N. Busschaert, L.E. Karagiannids, M. Wenzel, C.J.E. Haynes, N.J. Wells, Philip G. Young, D. Makuc, J. Plavec, K.A. Jolliffe and P.A. Gale, *Chem. Sci.* 2014, **5**, 1118.
28 W. F. Drew Bennett, Justin L. MacCallum and D. Peter Tieleman, J. Am. Chem. Soc., 2009, **131**, 1972.
29 a) A.V. Hill, *Biochem. J.*, 1913, **7**, 471; b) S. Bhosale and S. Matile, *Chirality*, 2006, **18**, 849.
30 S. J. Coles and P. A. Gale, *Chem Sci.*, 2012, **3**, 683.